Spin selection rules in single-electron transport through a few-electron quantum dot

T. Fujisawa[1,*], **D. G. Austing**[1,2], **Y. Tokura**[1], **Y. Hirayama**[1,3], **and S. Tarucha**[1,4,5]

[1] NTT Basic research Laboratories, NTT Corporation
3-1, Morinosato-Wakamiya, Atsugi, 243-0198, Japan.

[2] Institute for Microstructural Sciences M23A, National Research Council of Canada, Ottawa, Ontario K1A 0R6, Canada.

[3]CREST, 4-1-8 Honmachi, Kawaguchi, 331-0012, Japan.

[4] University of Tokyo, Bunkyo-ku, Tokyo, 113-0033, Japan.

[5] ERATO Mesoscopic Correlation Project, 3-1, Morinosato-Wakamiya, Atsugi, 243-0198, Japan.

[*] Corresponding author. E-mail: fujisawa@will.brl.ntt.co.jp

Abstract. Since a quantum dot has an extremely long spin relaxation time, we must consider two spin selection rules for its transport characteristics. Namely, the total spin of the quantum dot is conserved during internal transitions, and it should change by ±1/2 during a single-electron tunneling transition. We find that these selection rules are strictly obeyed in transport through a few-electron vertical quantum dot, and that related non-equilibrium transport can break the single-electron tunneling scheme.

1. Introduction

A quantum dot (QD) in the Coulomb blockade (CB) regime has discrete many-body energy states with a well-defined total spin, S, for a well-defined electron number, N [1]. This characteristic is attractive for the manipulation of the spin and charge state of electrons. The spin relaxation time in a QD is an important parameter for spin-memories and quantum information storage [2,3]. The inelastic spin relaxation time is theoretically predicted to be much longer than 100 μs for a typical GaAs QD [4]. Actually, the relaxation time can easily exceed the experimental limit of conventional optical and electrical measurements [5,6]. Our recent electrical measurements reveal an extremely long spin-flip energy relaxation time, $\tau_{spin} > 100$ μs. This is much longer than the typical interval for tunneling events ($\Gamma^{-1} = 1$ - 100 ns for a typical tunneling current of $e\Gamma \sim 1$ - 100 pA, where Γ is the tunneling rate), as well as the momentum relaxation time, $\tau_{mo} \sim$ 10 ns [7,8]. Therefore, no internal transition that changes the total spin of the QD occurs within the typical transport time scale.

There is another important selection rule in the transport characteristics, and it is responsible for the spin-blockade effect. Since a single electron possesses a spin 1/2, a single-electron tunneling transition should change the total spin by ±1/2, and other

tunneling transitions should be forbidden [9]. The spin blockade effect has been discussed for the suppression of the conductance or the appearance of negative-differential conductance [10,11,12]. However, most of the experimental interpretations for the weak suppression of the conductance seem to contradict the naïve expectation of a complete suppression of the current.

In this article, we investigate these spin-selection rules (the spin conservation and the spin blockade effect) in the transport characteristics of a few-electron QD. All the transport processes can be well understood by these spin selection rules. *However*, we find that the number of electrons, the total spin, and the total energy of the QD can fluctuate significantly due to non-equilibrium transport. Although our findings for a few-electron QD are obtained from gate-voltage pulse excitation measurement, the same tunneling transitions can also be seen in conventional dc transport characteristics.

2. Reconsideration of orthodox Coulomb blockade theory

Figure 1(a) shows the allowed tunneling transitions between different (N, S) states in a few-electron QD consistent with the two kinds of spin selection rules. For example, the internal transition between (N, S) = (2, 0) and (2, 1) (dotted arrow) is forbidden by spin conservation. The tunneling transition between (N, S) = (2, 0) and (3, 3/2) (dashed arrow) is forbidden by the spin blockade. These spin selection rules restrict the possible transitions in a QD, and give rise to complicated excitation processes that cannot be explained by orthodox CB theory.

The orthodox CB theory accounting for the CB effect and single-electron tunneling (SET) was originally introduced for transport through a small conductive island with a continuum density of states [13]. This theory is widely accepted for a variety of systems involving semiconductors, normal and superconducting metals, and molecules. The total energy, $U(N)$, of the system, in which an island containing N electrons is electrostatically affected by a gate voltage, V_g, via a capacitance, C_g, is given by

$$U(N) = \frac{(-Ne + C_g V_g + q_0)^2}{2C_\Sigma} + E_{\text{int}}(N). \quad (1)$$

The first term is the electrostatic energy approximated by a constant Coulomb interaction. Enclosed in the parenthesis is the sum of the electron charge on the dot, the induced charge by the gate, and an offset charge, q_0. C_Σ is the total capacitance of the dot. The second term, $E_{\text{int}}(N)$, is the sum of the energies of the occupied N electron levels, measured relative to the Fermi energy of the leads, accounting for the internal degrees of freedom of the QD. Other corrections to the many-body interactions are also included in E_{int}. In the orthodox theory, as originally considered for a continuum density of states, the second term is neglected because the QD is assumed to relax quickly to the minimum energy, E_{int}^{min}, which is almost independent of N. In this SET scheme, an electron that has entered the island leaves before another electron is allowed to enter when $U(N_0) = U(N_0+1)$ as shown in Fig. 1(b). This situation is maintained unless the excitation energy exceeds the charging energy, $E_c = e^2/C_\Sigma$. In this picture, spin is neglected and N-electron ground states (GSs) are only considered.

For a QD, in which energy quantization and many-body interactions are significant, we must consider the discrete energy of the dot, $E_{\text{int}}(N, S, M)$, which is characterized by total spin, S, and total angular momentum, M [1]. We focus on the regime $\tau_{\text{spin}} >> \Gamma^{-1}$, τ_{mo}, where spin-flip energy relaxation is effectively absent. This is the typical condition for a

dot weakly coupled to the leads, i.e. the coupling to the leads is still strong enough to give a measurable current ($e\Gamma > 1$ fA), but weak enough to prevent cotunneling current. If the QD is excited to any N-electron state with a different total spin from that of the N-electron GS, the excited state (ES) cannot always relax to the GS before the QD undergoes a tunneling transition to another $N \pm 1$ electron state [14-16]. Successive tunneling transitions force the QD into highly non-equilibrium configurations. Figure 1(c) shows a particular $U(N, S)$ diagram, which can actually be realized in our QD (see below). Long-lived ESs are now included, and the different spin states have different energies because of Coulomb interactions. The allowed tunneling transitions indicated by the arrows require excitation energies smaller than the addition energy, E_a. All these transitions can cause the dot state (N, S, and U) to fluctuate dramatically.

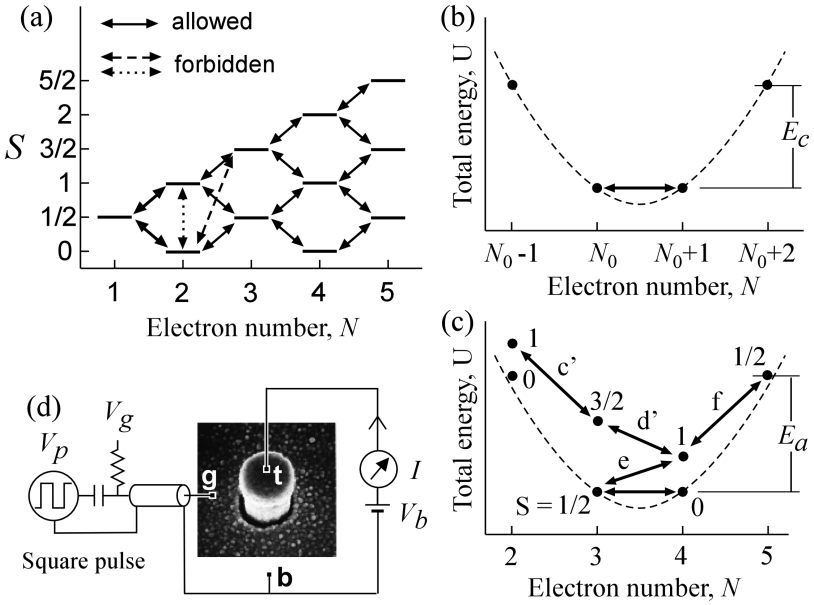

Fig. 1 (a) Possible total spin, S, for various numbers of electrons, N, in a QD. The solid arrows indicate allowed tunneling transitions, in which S changes by 1/2. Other transitions are forbidden by spin blockade (a representative transition is indicated by the dashed arrow) or by spin conservation (dotted arrow). (b) Total energy $U(N)$ of a small classical island when SET allows N to fluctuate between N_0 and N_0+1. (c) $U(N, S)$ for the QD at a particular condition (at the gate voltage γ in Fig. 2). The arrows indicate allowed tunneling transitions with excitation energy smaller than the addition energy, E_a. (d) Schematic setup for the pulse measurement on a vertical QD. The circular pillar is 0.54 μm in diameter. All the measurements are performed at a temperature ~ 0.1 K. The magnetic field is applied parallel to the current.

3. Pulse-excited current spectra

A few-electron vertical QD was fabricated in an AlGaAs/InGaAs heterostructure to study the spin selection rules and non-equilibrium transport [17,18]. Electrons are confined laterally by an approximate two-dimensional harmonic potential (confinement energy of about 4 meV). The N-dependent addition energy clearly reveals a shell structure for a circular disk-shaped QD. The quantum numbers, N, S and M can be

identified from the magnetic field, B, dependence of the current spectrum. Zeeman splitting is not resolved, so we neglected it.

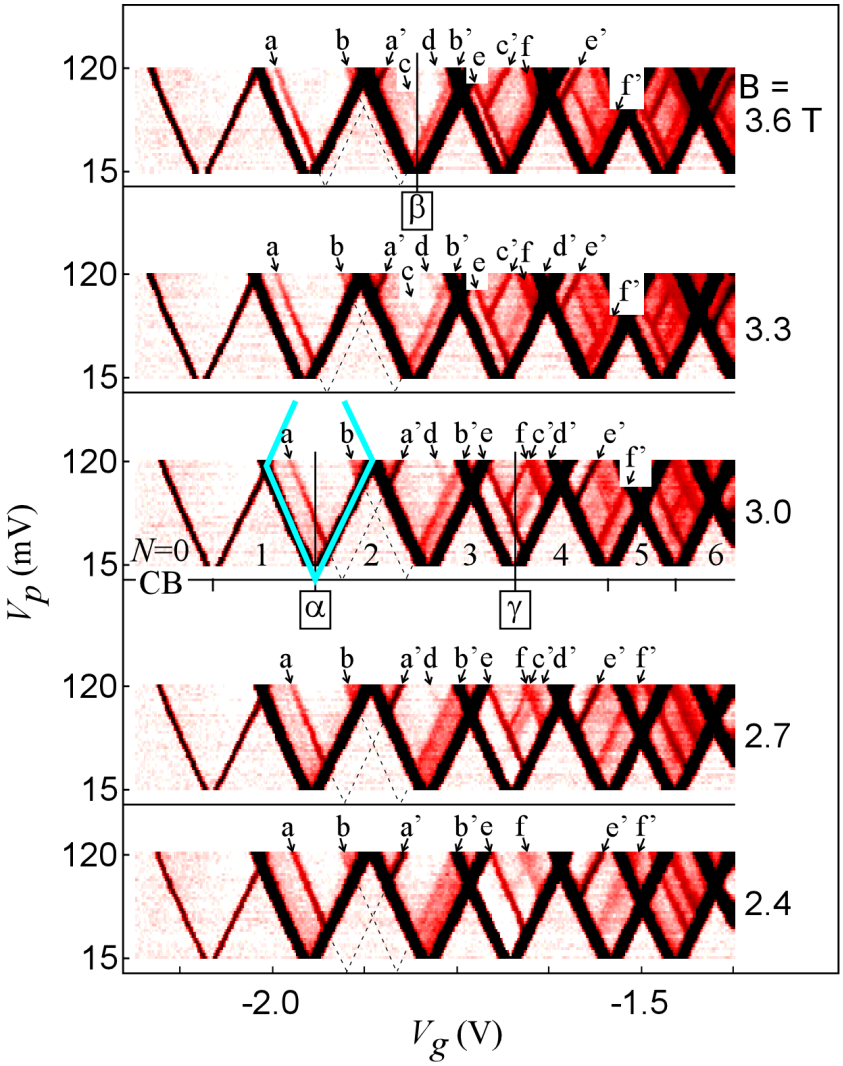

Fig. 2 (color). Pulse excited current spectra measured from B = 2.4 T (the bottom spectrum) to 3.6 T (the top spectrum). The colors represent current amplitudes [white (0 pA) - red (0.25 pA) - black (≥ 0.5 pA)]. N is fixed in each triangular region along the bottom due to CB. The pulse excited current through long-lived ESs is marked by arrows a, a', b, b', etc. The prime (non-prime) indicates a transition that decreases (increases) N by one.

To investigate highly non-equilibrium transport, we employ a pulse excitation technique [6,7,19]. A square pulse of amplitude V_p, combined with the static gate voltage, V_g, is applied to the gate electrode (g) as shown in Fig. 1 (d). A small dc bias voltage V_b = 0.15 mV is also applied so that electrons are injected from the bottom contact, b (corresponding tunneling rate, $\Gamma_b^{-1} \sim 10$ ns), and escape to the top contact, t ($\Gamma_t^{-1} \sim 100$ ns). The averaged dc current, I, is measured during the gate-voltage pulse irradiation.

The pulse-induced transport involving any ES is strongly affected by the energy relaxation time of the ES. If the conditions are adjusted in such a way that $\tau_{spin} >> \Gamma_t^{-1}$, t_p, $\Gamma_b^{-1} >> \tau_{mo}$, one can *only* study current associated with long-lived spin states, whose total spin is different from that of any lower-lying states [16,19]. Therefore, only the lowest-energy state for any given N and S need be considered for the pulse-excited current, and

other short-lived states can be neglected. This technique is very useful in the analysis, as will be seen below.

Figures 2 show the pulse-excited current spectra for N = 0 to 6 for B = 2.4 to 3.6 T. For each spectrum, each current peak initially observed in the absence of the pulse ($V_p \sim$ 0 V) is due to the SET transition between the N- and (N+1)-electron GSs, and splits into two peaks of equal height (truncated in the color scale), when the pulse is applied. Weaker additional peaks, indicated by the arrows are due to transient current through long-lived ESs. Rich structure is observed in the current spectra for B = 2 to 4 T, where various many-body spin states are energetically close to one other [17]. The representative spectra in Fig. 2 are observed in the B range where the GS of the N-electron QD is spin-unpolarized (i.e., the smaller-S states have lower energy).

There are a number of general features observed in the spectra. First, when the peak positions are extrapolated to lower V_p, pairs of peaks (e.g. labeled a and a') meet at V_p = 0 V exactly (see e.g. dashed lines for pairs a-a' and b-b'). This behavior can be seen for all peaks and for the entire magnetic field range (0 - 6 T) we investigate. The peaks in Fig. 2 are labeled in such a way that the prime (non-prime) labeled peaks are associated with tunneling transitions during the low (high) phase of the pulse. Second, some of the current peaks are terminated by other current peaks (e.g. peak d is terminated by peak b', and peak d' by peak e). This will be discussed in the next section. Third, the number of peaks is more than that expected for a simple SET scheme. For example, as shown in Fig. 1(a), there are only two possible allowed tunneling transitions between long-lived states in a N = 1 and 2 QD. However, in total, three peaks (a and b and the SET peak) are seen in the conductive region between the N = 1 and 2 CB regions. Peak b cannot be explained by a higher-lying short-lived excited state of the N=2 QD. It can only be explained by considering non-equilibrium tunneling processes.

4. Non-equilibrium tunneling transitions

All the transport spectra in Fig. 2 can be well understood from the total energy diagrams in Fig. 3. Figure 3(a) is the $U(N, S)$ diagram when the gate voltage is set to position α at B = 3.0 T in Fig. 2. SET between (N, S) = (1, 1/2) and (2, 0) is always possible even at zero excitation energy. The single-particle excitation to (2, 1), corresponding to peak a in Fig. 2, becomes possible when the excitation energy exceeds the level spacing, Δ_2. Since the energy relaxation from (2, 1) to (2,0) is forbidden due to spin-conservation, the (2, 1) state is stable until another tunneling transition takes place. Then, the QD can be excited to charge state (3, 1/2), indicated by the double-lined arrow in Fig. 3(a). This excitation requires the energy of E_a - Δ_2, which is considerably smaller than the addition energy E_a. Since the excitation to (3,1/2) involves three charge states, N = 1, 2 and 3, this tunneling process can be thought of as novel double-electron tunneling (DET). The corresponding current peak is labeled b in Fig. 2. At gate voltage α, this novel DET process would require $V_p \sim$ 200 mV, which is beyond the range of Fig. 2. However, it is clear that peak b should appear inside the blue bounded diamond-shaped region in which SET is expected from orthodox theory, as indeed it does. Figure 3(b) is the $U(N, S)$ diagram when the gate voltage is adjusted to β in Fig. 2. The SET between the N = 2 and 3 GSs, single particle excitation to (N, S) = (2, 1) (peak b' in Fig. 2 and corresponding transition labeled b' in Fig. 3(a)), and novel double electron tunneling into (1,1/2) (peak a') are clearly seen. The extra peak c, although it is faint, is attributed to the transition from (2, 1) to (3, 3/2). This tunneling process is called here ES-ES tunneling,

because no GSs are involved. This highly non-equilibrium transport is possible because the spin-flip energy relaxation from (2, 1) to (2, 0) is forbidden. Since this ES-ES excitation requires a "pre-excitation" from (3, 1/2) to (2, 1) (labeled b'), transition c can only appear when transition b' is possible. So the corresponding current peak, c in Fig. 2, is terminated by peak b'. Similar "terminations", such as peak d terminated by peak b', peak c' by peak e, and peak d' by peak e, are clearly seen in Fig. 2. They are all attributed to ES-ES tunneling.

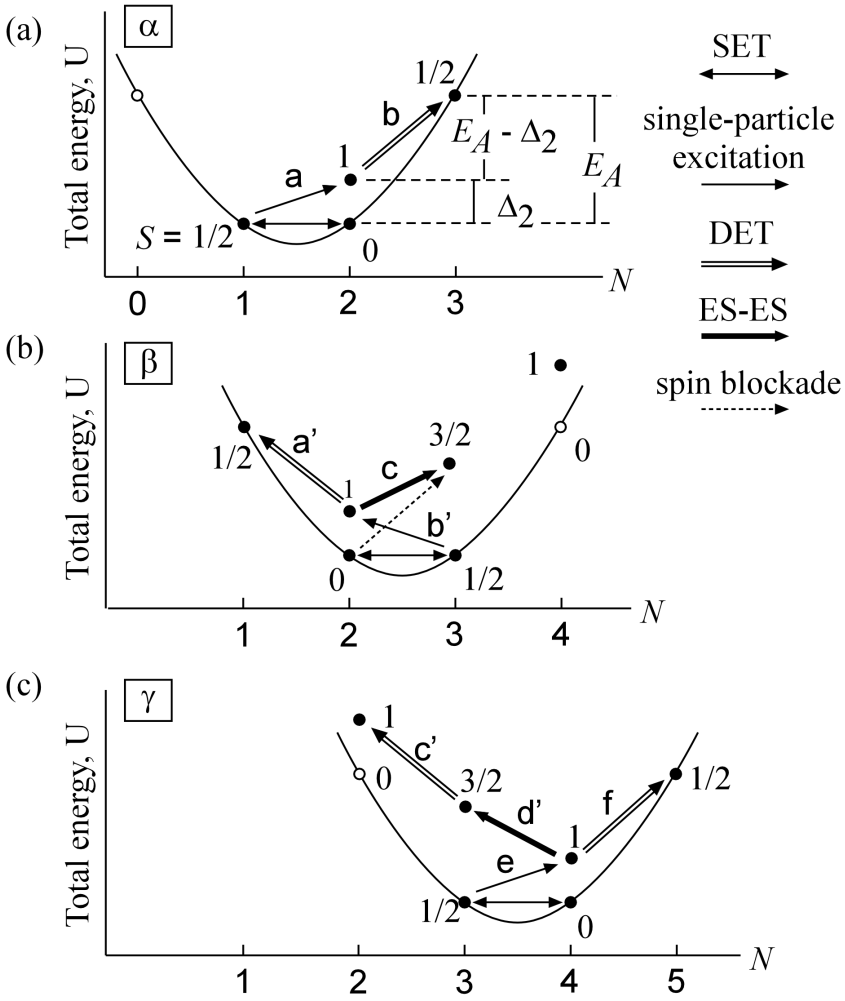

Fig. 3. Total energy diagrams U(N,S). (a), (b), and (c) respectively account for tunneling transitions at the gate voltage α, β, γ in Fig. 2. The numbers in the figures are the total spins of the states. Arrows identify possible single-electron tunneling transitions. These are single-electron tunneling (SET) between the *N* and *N*+1 GSs (thin double headed arrow), single particle excitation from a GS to an ES (thin arrow), novel double-electron tunneling (double-lined arrow), tunneling between two ESs (thick arrow), and spin-blockaded (dashed arrow, forbidden). All transitions except those spin-blockaded are observed.

It should be noted that the transition from (2, 0) to (3, 3/2) at β in Fig. 3(b) is not observed because of spin-blockade. A closer look at the *B*-dependence is required in order to clearly see that the origin of peak c is in Fig. 2 is ES-ES tunneling from (2, 1), and not the broken spin-blockaded transition from (2, 0). The difference between the two

cases should appear in the gate voltage dependence of the current peak, when the energies of the two corresponding states are nearly degenerate. Figure 4(a) shows the B-dependence of the peak positions for the SET peak between the $N = 2$ and 3 GSs (solid circles), and for one of the pulse-excited current peaks (open circles). The SET peak position shows some kinks related to the level crossings of $N = 2$ or 3 GSs. From a comparison with an exact diagonalization calculation shown in Fig. 4(b) [20], we can identify a transition from a spin-singlet ($S = 0$) to a spin-triplet ($S = 1$) of the $N = 2$ QD at $B = B_{S\text{-}T}$, a momentum transition from $M = 1$ to $M = 2$ of the $N = 3$ QD at $B = B_M$, and a transition from the spin-doublet ($S = 1/2$) to spin-quadruplet ($S = 3/2$) of the $N = 3$ QD at $B = B_{D\text{-}Q}$. The excited state peaks (open circles) follow the crossing behavior with respect to the doublet-quandrupted GS transition at around $B \sim B_{D\text{-}Q}$. Now suppose we look at the peak position of the pulse-excited current below $B = B_{S\text{-}T}$. If the current arises from the transition (N, S) = (2, 0) to (3, 3/2), violating spin-blockade, the peak position should show a kink at $B = B_{S\text{-}T}$ due to the GS level crossing of the $N = 2$ QD, and follow the blue dotted line in Figs. 4(a) and 4(b). However, the peak position does not show any kink at $B \sim B_{S\text{-}T}$, and follows the red solid line smoothly. This is expected for ES-ES tunneling from (2, 1) to (3, 3/2). Therefore, the current peak at $B < B_{S\text{-}T} \sim 4$ T must be associated with ES-ES tunneling. Actually, we never see the spin-blockaded transition within our current sensitivity (~ 1 fA).

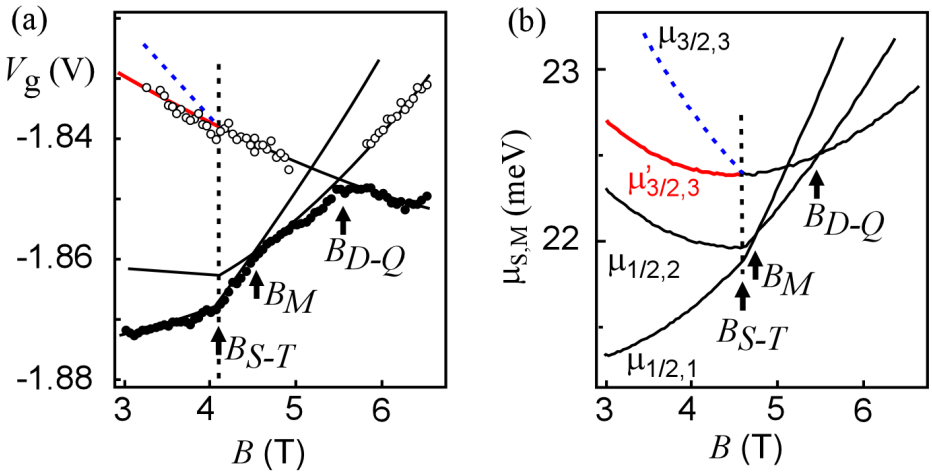

Fig. 4. (a) The gate voltage dependence of the pulse-excited current peaks. Solid circles are for the SET current between the $N = 2$ GS and $N = 3$ GS, while open circles are for pulse-excited current involving a long-lived ES. (b) Electrochemical potential, $\mu_{S,M}$, calculated by an exact diagonalization calculation for the tunneling transitions to the $N = (3, S, M)$ states. The black solid lines are calculated with $\mu_{S,M} = U(N{=}3, S, M) - \min[U(2,0), U(2,1)]$. The blue dashed line is for the spin-blockaded transport, $\mu_{3/2,3} = U(N = 3, S = 3/2, M = 3) - U(2, 0)$, while the red solid line is for the ES-ES tunneling, $\mu'_{3/2,3} = U(N{=}3, S{=}3/2, M{=}3) - U(2, 1)$. The corresponding lines in (a) are guides for the eye only.

Other complex tunneling processes involving both novel DET and ES-ES tunneling are also observed. Peak d (c') in Fig. 2, which is terminated by peak b' (e), is attributed to ES-ES tunneling, whose excitation process involves three charge states. More complicated excitations are expected for QDs with more electrons. Four different peaks (e, f, c' and d' in Fig. 2) are observed between the $N = 3$ and 4 CB regions. The corresponding transitions are indicated in the total energy diagram in Fig. 3(c). The

fluctuation in the total energy can be significantly greater than the pulse excitation energy. Non-equilibrium transport can lead to the accumulation of energy in excess of the excitation energy. As N increases, many long-lived ESs with different S can contribute to the transport. The complexity of many-body excitations is expected to increase with N and S [21].

5. Summary

We successfully investigated tunneling transitions associated with long-lived spin states. All the tunneling processes are understandable in terms of spin selection rules (spin conservation and spin blockade). However, non-equilibrium transport causes significant fluctuation of the number of electrons, total spin, and total energy of the QD. It is important to suppress these non-equilibrium tunneling processes for the easy manipulation of spin and charge in a QD. For example, the charging energy (or addition energy) is no longer a good index since the SET scheme is no longer simply followed. In order to keep in the true SET regime, any excitation energy (applied voltage, thermal energy, etc.) has to be minimized to avoid double-electron tunneling.

References

[1] L.P. Kouwenhoven et al., Reports on Progress in Physics 64, 701 (2001).
[2] D. Loss and D.P. DiVincenzo, Phys. Rev. A 57, 120 (1998).
[3] P. Recher, E.V. Sukhorukov, and D. Loss, Phys. Rev. Lett. 85, 1962 (2000).
[4] A.V. Khaetskii and Yu.V. Nazarov, Phys. Rev. B 61, 12639 (2000).
[5] M. Paillard, et al., Phys. Rev. Lett. 86, 1634 (2001).
[6] T. Fujisawa, Y. Tokura, and Y. Hirayama, Phys. Rev. B 63, 081304(R) (2001); ibid Physica B 298, 573 (2001).
[7] T. Fujisawa et al., to be published.
[8] U. Bockelmann, Phys. Rev. B 50, 17271 (1994).
[9] D. Weinmann et al., Phys. Rev. Lett 74, 984 (1995).
[10] L.P. Rokhinson, et al., Phys. Rev. B 63, 035321 (2001).
[11] A.K. Huttel et al., cond-mat/0109104.
[12] M. Ciorga et al., Appl. Phys. Lett. 80, 2177 (2002).
[13] H. van Houten, C.W.J. Beenakker and A.A.M. Staring, in "Single Charge Tunneling, Coulomb Blockade Phenomena in Nanostuctures" ed. H. Grabert and M.H. Devoret, NATO ASI series B 294 (Plenum Press, New York, 1991), pp. 167-216.
[14] J. Weis et al., Phys. Rev. Lett. 71, 4019 (1993).
[15] O. Agam et al., Phys. Rev. Lett. 78, 1956 (1997).
[16] T. Fujisawa et al., Phys. Rev. Lett. 88, 236802 (2002).
[17] S. Tarucha et al., Phys. Rev. Lett. 77, 3613 (1996).
[18] L.P. Kouwenhoven et al., Science 278, 1788 (1997).
[19] T. Fujisawa et al., Physica B 314, 224 (2002).
[20] S. Tarucha et al., Physica E 3, 112 (1998).
[21] B.L. Altshuler et al., Phys. Rev. Lett. 78, 2803 (1997).